Materials Science and Engineering C 70 (2017) 1095–1106

Contents lists available at ScienceDirect

Materials Science and Engineering C

journal homepage: www.elsevier.com/locate/msec

Functionalization of 2D transition metal dichalcogenides for biomedical applications

Zibiao Li, Swee Liang Wong *

*Institute of Materials Research and Engineering, A*STAR (Agency for Science Technology and Research), 2 Fusionopolis Way, Innovis #08-03, 138634, Singapore*

ARTICLE INFO

Article history:
Received 22 January 2016
Received in revised form 4 February 2016
Accepted 14 March 2016
Available online 15 March 2016

Keywords:
Transition metal dichalcogenides
Two-dimensional
Biomaterials
Biomedical applications
Biosensor
Functionalization

ABSTRACT

Recent research has revealed a gamut of interesting properties present in layered two-dimensional (2D) transition metal dichalcogenides (TMDCs) such as photoluminescence, comparatively high electron mobility, flexibility, mechanical strength and relatively low toxicity. The large surface to area ratio inherent in these materials also allows easy functionalization and maximal interaction with the external environment. Due to its unique physical and chemical properties, much work has been done in tailoring TMDCs through chemical functionalization for use in a diverse range of biomedical applications as biosensors, drug delivery carriers or even as therapeutic agents. In this review, current progress on the different types of TMDC functionalization for various biological applications will be presented and its future outlook will be discussed.

1. Introduction

Two-dimensional (2D) materials have received much attention since the seminal paper on graphene in 2004 [1]. Intensive efforts from both academia and industry have been placed in the research of these materials [2–6] due to their potential applications in various fields such as nano-electronics [7,8], energy storage, optoelectronics [7,8] and in biological systems [9–12]. In particular, due to their compatibility with existing biomedical materials and low cytotoxicity, together with superior physical and electronic properties, one class of 2D materials, TMDCs are seen as potential candidates for applications in biotechnology. In this review, we will focus on TMDCs, a layered material made up of stacked planar crystals with the chemical composition, MX_2, where M and X represent the central transition metal atom and the surrounding chalcogen atoms (Mo, S, Se) respectively, as shown in Fig. 1 [13,14]. Atoms of the same layer are covalently bonded in a hexagonal lattice while adjacent layers are held by weak van der Waals forces, allowing thinning of the stack to easily take place. Typical examples of some TMDCs being actively researched on include MoS_2, WS_2, WSe_2 and $MoSe_2$ etc. Depending on the elements involved as well as the structural arrangement between different physical phases, their electronic properties will vary, allowing flexibility in their potential applications [14]. Recently, TMDCs have seen an increased uptake in a variety of biomedical applications, such as drug delivery agents [15–19], therapeutics [15–21], bio-imaging [15–18,20–23] elements as well as biosensors [24–53] and therefore will be the materials of choice for this review.

Due to their large surface-to-volume ratio, TMDCs provide an easy to access platform for chemical functionalization to tailor its characteristics, for different requirements. Thus, it is essential to understand the various functionalization strategies or approaches which enable TMDCs to fulfill different purposes. Herein, we will present the recent developments in the functionalization of TMDCs for biomedical uses. The structural and electronic properties of TMDCs which make them compelling candidates for bio-related systems will be discussed and the various synthesis methods of the material will be touched on. Following which, an in-depth look on the different functionalization strategies or approaches of TMDCs and their associated applications will be presented. We aim to provide the readers an overview of the latest advances in functionalization of TMDCs for biomedical purposes as well as an outlook for future research.

2. Basic properties of TMDCs

Due to its layered structure (Fig. 1) and having only weak interplanar Van der Waals forces holding these layers together, TMDCs can be easily thinned down to a single molecular plane made up of 3 atoms in the vertical dimension (≈0.7 nm height), exhibiting a truly two-dimensional nature [13,14]. Due to its planar characteristic, TMDCs exhibit a very large surface-to-volume ratio which accommodates straightforward access for large area functionalization. The relatively large surface area also allows maximal interaction with the target biomaterial for increased efficiency as well as sensitivity in the

* Corresponding author.
E-mail address: wongsl@imre.a-star.edu.sg (S.L. Wong).

http://dx.doi.org/10.1016/j.msec.2016.03.039
0928-4931/

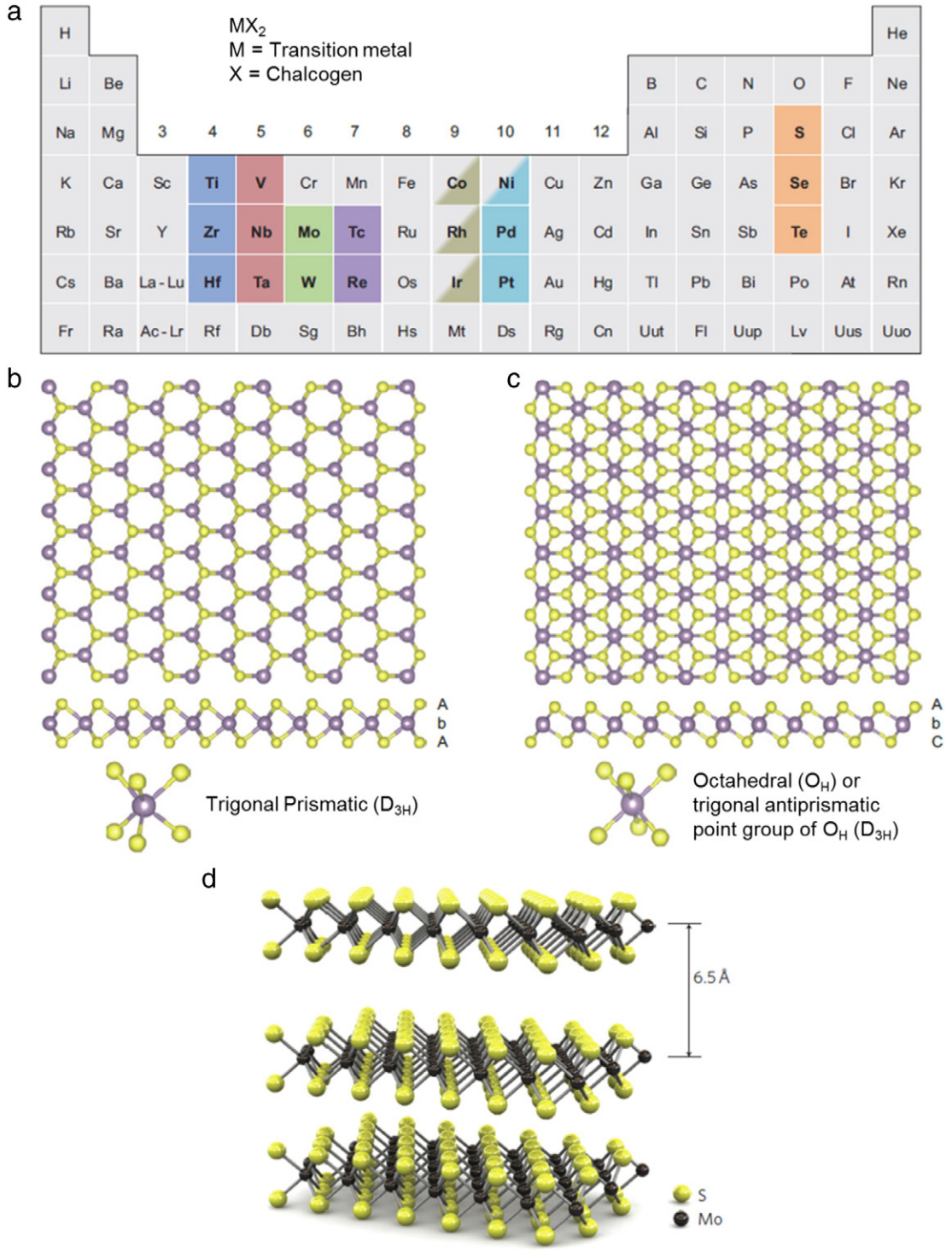

Fig. 1. Structure of monolayered TMDs. a) About 40 different layered TMD compounds exist. The transition metals and the three chalcogen elements that predominantly crystallize in those layered structure are highlighted in the periodic table. Partial highlights for Co, Rh, Ir and Ni indicate that only some of the dichalcogenides form layered structures. c-Axis and section view of single-layer TMD with trigonal prismatic (b) and octahedral (c) coordinations. Atom color code: purple, metal; yellow, chalcogen. The labels AbA and AbC represent the stacking sequence where the upper- and lower-case letters represent chalcogen and metal elements, respectively. d) Three-dimensional representation of the structure of MoS_2 with single layers being 6.5 Å thick. Panels a), b) and c) are reproduced with permission from Ref. [14]. Copyright 2013, Macmillan Publishers Limited. Panel d) is reproduced with permission from Ref. [13]. Copyright 2011, Macmillan Publishers Limited.

case of sensing and imaging. Furthermore, there are no dangling bonds present on its intrinsic basal surface, allowing high stability in both air and liquids as it does not readily react with ambient chemicals [14]. This stability is retained even when their lateral dimensions are reduced to the order of tens of nanometers [54]. Such stability allows these materials to be easily introduced into biological systems for biomedical purposes or exposed to their associated environments for external diagnostics.

TMDCs are semiconducting and possess an electronic band gap which increases with decreasing thicknesses [8]. Coupled with considerable charge carrier mobilities, it enables TMDCs to be used in field-effect transistors as biosensors where changes in conductance when

exposed to the target analytes allow monitoring of their concentrations. Compared to graphene which has no electronic band gap, higher sensitivities can be reached due to a larger current on-off ratio which enhances the signal-to-noise ratio (SNR). In addition, as the layered crystal is thinned down to a single monolayer, it experiences a transition from an indirect electronic band gap to a direct electronic band gap [8]. This results in a significant increase in photoluminescence (PL) yield of monolayer TMDC as compared to its thicker counterparts. As 2D TMDCs are atomically thick, they are highly sensitive to external elements and the variation in PL strength in the presence of specific environments can be exploited for these materials to act as biosensors [9–12,22,36,55]. Electrochemical responses of these materials are also very sensitive to external perturbations and therefore can also function as a parameter for bio-sensing [24,29,31,37,38,41].

Due to their electronic band structure, TMDCs also exhibit strong optical absorption in the near-infrared (NIR) region (≈800 nm), higher than that of graphene oxide and its extinction coefficient is also better than that of gold nanorods [56]. These properties allow TMDCs to be efficient photothermal agents for use in drug delivery or therapeutic purposes as NIR lasers can efficiently penetrate through tissues with depth of several centimeters while having low tissue absorption. Presence of such photothermal agents enhances the selectivity of the excitation laser, allowing generation of heat in targeted areas (e.g. at tumor tissue) for therapeutic or drug release purposes while lowering the power density of laser required [11]. Suspensions of TMDCs such as MoS_2 with low concentrations of 100 s of ppm can reach temperatures >80 °C when exposed for several minutes to NIR radiation (≈800 nm, 0.8 W cm^{-2}) [11].

3. Synthesis of 2D TMDCs

2D TMDCs can be produced through both top-down and bottom-up means. In top-down processes, they can be fabricated by thinning down bulk TMDCs crystals to its constituent layers. The most commonly used method is mechanical exfoliation where an adhesive tape is used to peel off thin layers of TMDCs and deposit them on the desired surface [13]. Crystal quality of the material produced as such is the highest but is greatly limited by the randomness in thicknesses of the flakes that can be obtained as well as its low yield which prevents potential scaling up. However, 2D TMDCs obtained in this manner are well-suited as on chip sensors due to their enhanced sensitivity to environmental perturbations by virtue of their good electronic and physical quality [25–27]. An alternative liquid/chemical based exfoliation method has been demonstrated to achieve much larger quantities from bulk TMDCs crystals or powders, albeit with much smaller physical dimensions (<10 μm) and lower crystal quality [57]. In this process, the bulk materials are mixed with specific chemicals in solution and undergo external perturbation such as ultra-sonication to expand the interlayer spacing, resulting in eventual exfoliation of the material into its constituent layers. An advantage of this process would be the ability to introduce additional dispersants or intercalants into the system, allowing functionalization of the TMDC nanomaterial obtained during the exfoliation process. Furthermore, depending on the type of functionalization, the resulting nanomaterial can be made water soluble, allowing direct introduction of these materials into biological systems.

Bottom-up techniques for growth of 2D TMDCs include chemical vapor deposition (CVD) in which solid powders containing the elements present in the TMDC are thermally evaporated and undergoes chemical reaction on a solid surface to form the desired TMDC layer in a furnace at high temperatures [58–60]. As an example, for MoS_2 growth, MoO_3 and S powders are placed in a tube furnace in the presence of substrates such as SiO_2 or sapphire and are heated to temperatures of about 800 °C. The vapors formed from the evaporated powders then react to produce layered MoS_2 on the SiO_2 surface, with thicknesses dependent on the growth parameters such as carrier gas flow, reactant quantities, etc. Other bottom up techniques include introduction of chalcogen vapor to react with pre-deposited metallic films. The specifics of these techniques will not be covered here and the reader is encouraged to look up review articles [58–60] on fabrication methods for a more comprehensive overview. The resultant product of such bottom-up methods generally covers a much larger area than top-down exfoliation methods as they do not depend on thinning of bulk crystals and also allows controlled thicknesses to be grown, advantageous for large scale device fabrication.

2D TMDCs produced from bottom-up or mechanical approaches are normally used in external diagnostic applications rather than in vivo ones as the produced layers are much larger in size and are formed on solid substrates, unlike liquid exfoliation where the formed products are in solution. All of the above mentioned fabrication methods have their individual drawbacks and advantages. The choice of method depends on the particular system in which the 2D TMDC is applied. Factors of consideration include costs, required quantity/area, desired level of crystal quality, biocompatibility, specific modifications of the nanomaterial required as well as the eventual environment that the material would be placed in. As we delve into the various types of functionalization and their associated applications in the following sections, the choice of fabrication would be made clear.

4. Functionalization of TMDCs for biomedical applications

As introduced in the previous sections, atomically thin TMDCs possess a wide array of useful properties such as high photothermal response, fluorescence and moderate conductivity that can be exploited for a range of biomedical applications. However, these materials are not intrinsically biocompatible and require additional functionalization if they are to be incorporated into biological systems. In addition, further functionalization may be required in order to enhance its sensitivity as a diagnostic tool or imbue the TMDCs with additional capabilities such as drug delivery, DNA sensing or contrast imaging. Due to their large surface to volume ratio, functionalization of TMDCs is relatively straightforward and can be either non-covalent or covalent.

Non-covalent functionalization is often carried out in TMDCs when keeping the intrinsic properties of the 2D TMDC is essential or removal of the functional groups off the TMDC is part of the diagnostic/delivery mechanism. Such functionalization generally involves physisorption of the desired probe or drug carriers onto the relatively large basal surface of the TMDC, allowing maximal loading as well as interaction with the surrounding environment. Covalent modification involves formation of chemical bonds of the chemical group to be functionalized on the TMDC surface. This can take place through specific reaction processes such as thiol chemistry for the case of sulfur based TMDCs [61,62]. Such covalent bonding is generally required to firmly anchor the functional groups on the TMDC surface as well as to alter the physical/electronic properties of the TMDCs. These modifications depend on the functional material that is introduced onto the TMDC. Polymers [15–18,41,42] or smaller organic molecules [23,25–27,29,30] can be covalently or non-covalently bonded to TMDCs for biosensing and therapeutic purposes. Probes functionalized onto TMDCs include single stranded fluorescent-labeled DNA whom luminescence is affected by its adsorption to the TMDC layer and subsequent hybridization with another DNA single strand [46,48–53].

Another form of modification involves decoration with metallic nanoparticles [15,31,39–43] that enhance the electrocatalytic ability of TMDCs or serve as contrast agents for imaging. Other non-covalent functionalization involves stacking of additional 2D materials [37,38,42,44,45] to increase its detection sensitivity. Pores can also be intentionally created in TMDCs for DNA sequencing purposes [32–34]. Depending on the modifications present on the TMDC and the interaction with external chemical elements, the response of the TMDC to changes in the environment varies and thus sets the basis for biomedical applications. A schematic [11] showing one such procedure and application is described in Fig. 2. In the following sections, different types of functionalization will

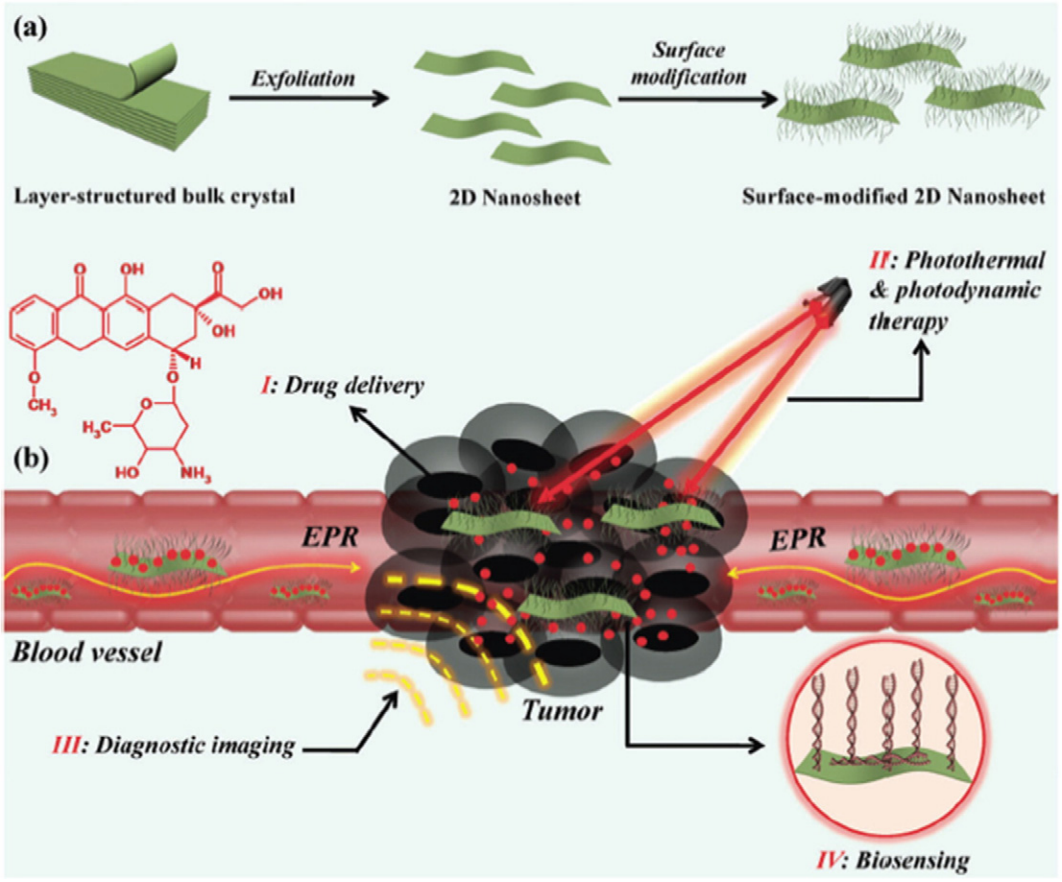

Fig. 2. a) Typical synthetic procedure for surface-modified 2D layered nanosheets by the typical top-down exfoliation approach. b) Schematic illustration of biomedical applications of 2D-graphene analogues against cancers, including drug delivery, photo/photodynamic therapy, diagnostic imaging and other specific applications such as biosensing. Reproduced from Ref. [11] with permission from The Royal Society of Chemistry. Copyright 2015, Royal Society of Chemistry.

be discussed according to the material types that are to be added to the TMDC and their respective applications will be discussed.

4.1. Polymers

Most 2D TMDCs do not form well-defined stable suspension in many common polar solvents such as water, thus making it difficult for in vivo applications [10]. To improve the stability of TMDCs in solution, especially for use in biological systems, additional functionalization is required. One form of functionalization involves the non-covalent addition of biocompatible polymers to these TMDC materials to form polymer/TMDC composites. These polymers are generally introduced into the system as a reagent during the intercalation process of bulk TMDCs for production of 2D nanosheets. The thus synthesized TMDC nanoflakes would therefore be well-functionalized with these polymers. In addition, these polymers can also serve as loading centers to further accommodate drug molecules. Drug loading to weight ratio (ratio between the weights of loaded drugs and TMDC) is reported, for the case of doxorubicin (DOX) which is a chemotherapy drug, in MoS_2, to be as high as 240% [19], larger than that of graphene oxide (140%) [63]. As mentioned previously, the relatively high NIR absorbance of these TMDCs such as MoS_2 allows them to be appropriate for photothermal based ablation of harmful cells. Furthermore, such a property can function as a trigger for release of chemotherapeutic agents from loaded drug carriers, allowing TMDCs to act as smart platforms for controlled therapeutic/drug release.

Demonstration of these capabilities has been performed by Liu et al. where 2D MoS_2 nanosheets are functionalized with polyethylene glycol (PEG) [19]. The polymer served dual functions, one to enhance nanosheet stability and biocompatibility while at the same time attaching folic acid for targeted entry into cancer cells. Using the synergy between the NIR photoablation provided by the nanosheets as well as DOX release from the functionalized nanosheets, successful suppression of tumor growth was achieved. Using chitosan coated MoS_2 nanosheets, Yin et al. also demonstrated NIR-triggered localized drug delivery of DOX and hyperthermia treatment of pancreatic cancer in vivo [18]. Likewise, other TMDCs like WS_2 [20] and TiS_2 [21] were also utilized similarly and they displayed comparable levels of efficiency and biocompatibility.

Shown in Fig. 3 is a recent example by Wang et al., in which poly(lactic-*co*-glycolic acid) (PLGA) is homogenized with MoS_2 and DOX in *N*-methylpyrrolidone (NMP) to form a multifunctional oleosol [17]. As PLGA is a hydrophobic polymer which undergoes a liquid-solid phase transformation in contact with water, it serves to encapsulate the MoS_2/DOX composite, allowing localized therapeutic implant. Compared to usual forms of functionalized TMDC nanosheets in suspension, this method allows in vivo tumor photothermal and chemotherapy to occur with low concentrations of photothermal agent (30 μg of MoS_2) and drug dosage (75 μg of DOX). In addition, the MoS_2 nanosheets and DOX are well-shielded, minimizing leakage into the bloodstream. In vivo efficiency of the composite implant for cancer therapy mouse mold is described in Fig. 3 (d_1–d_4). The generated photothermal response on NIR exposure results in both tumor coagulation necrosis as well as triggering of the encapsulated DOX molecules for increased chemotherapeutic efficiency. High NIR laser absorbance of the MoS_2 nanosheets also provides high performance contrast for imaging purposes [15,17,18].

Other cases of TMDC nanosheets acting as carriers also include photosensitizers for use in photodynamic treatment of diseases. Instead of using thermal energy as a source of carrier release stimuli or therapy,

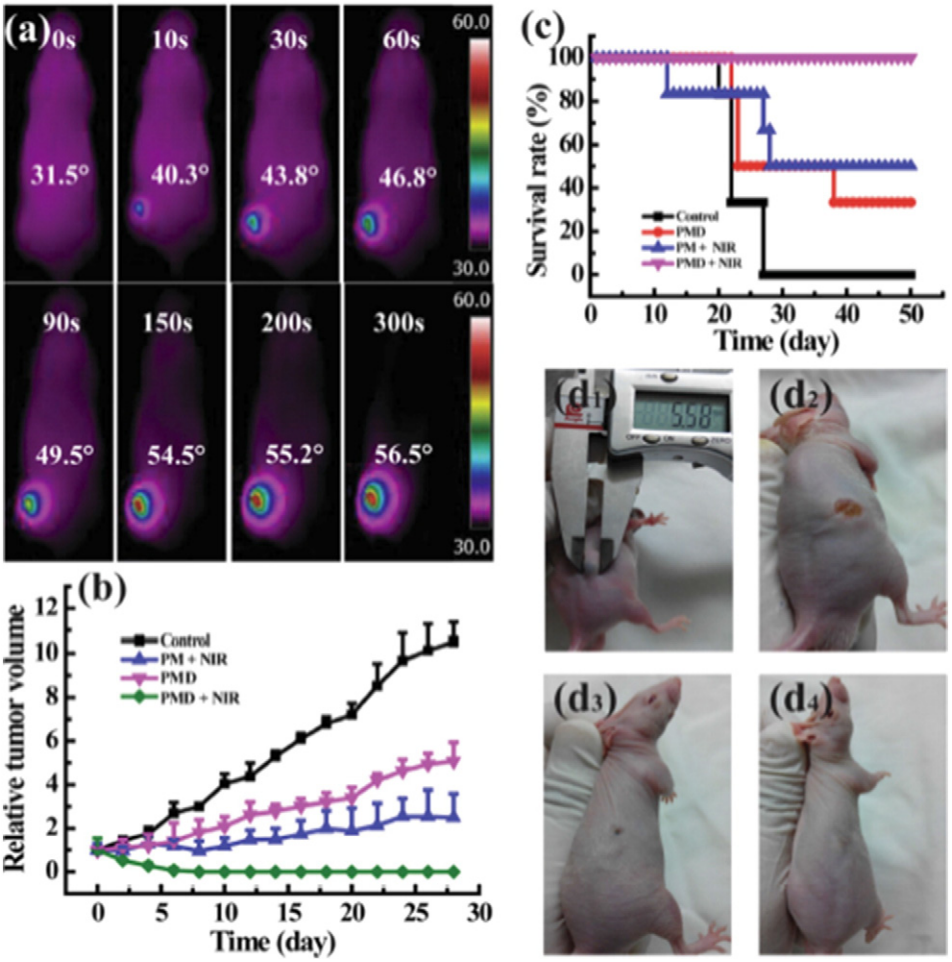

Fig. 3. In vivo therapeutic efficiency of PLGA/MoS_2/DOX oleosol (PMD) implant for cancer therapy. (a) In vivo thermal images of PMD-implanted mouse under continuous irradiation of 808 nm laser (0.6 W cm^{-2}) for varied durations. b) Tumor volume-changing profile of 4 T1 tumors after several treatments as described. c) The long-term survival rate of mice after different treatments. Panels (d_1–d_4) show the digital photos of PMD-implanted tumor-bearing nude mice after single laser irradiation for extended days. Reproduced with permission from Ref. [17]. Copyright 2015, WILEY-VCH Verlag GmbH & Co. KGaA, Weinheim.

light energy is utilized for creating singlet oxygen species for destruction of cells. TMDCs like WS_2 have been used in a combination of both photothermal and photodynamic treatment after functionalization with methylene blue, a photosensitive agent [20]. Thus, through use of suitable polymers to enhance compatibility and stability of TMDCs in biological systems as well as loading of drug carriers, one can exploit the unique properties of TMDCs such as high NIR absorbance for carrier release stimulation or as a direct source of therapy for a synergistic approach in physiological therapy. Furthermore, TMDCs can also act as contrast agent in X-ray computed tomographic imaging due to the strong X-ray attenuation ability caused by the presence of transition metals for simultaneous imaging diagnosis and therapy for biomedical applications [16,18,20].

4.2. Small organic molecules

An alternate functionalization choice would be smaller organic molecules such as acids [23,29], dyes [30] as well as bioreceptors [25–27]. Similar to polymers, they also allow aqueous solutions of TMDCs if these molecules possess hydrophilic groups such as hydroxyl or carboxyl species. An advantage over polymer-based functionalization would be their smaller physical dimensions, allowing cellular uptake for purposes such as cell labeling and drug delivery directly into cells. Fig. 4 describes such a schematic for the uptake of decorated TMDC nanosheet drug carriers and subsequent expulsion from biological cells [10]. Other usage includes enhancement of the electrocatalytic efficiency of the host TMDC platform through its electrostatic interaction with the attached molecules. Biosensors can also be fashioned from TMDCs based on the quenching/recovering of fluorescence from functional molecules due to environmental perturbations. Such molecules can be grafted onto TMDCs through simple physisorption/chemisorption or in certain cases, thiol chemistry [61,62] between the sulfur atoms present on the molecules and intrinsic sulfur vacancies in metal sulfides.

Recent report by Yang et al. demonstrates the use of MoS_2 as a non-toxic nanoprobe for detection of silver ions in aqueous solutions and living bacteria cells after the TMDC has been modified by fluorescent rhodamine B isothiocyanate (RhoBS) molecules [30]. After initial adsorption of RhoBS molecules on the MoS_2 nanosheets, their fluorescence is quenched due to Förster resonance energy transfer. In contact with Ag^+ ions, reduction of Ag^+ ions to nanoparticles occurs as well as detachment of the fluorescent RhoBS. This process leads to the recovery of the fluorescence intensity which is further surface enhanced by the presence of Ag nanoparticles thus allowing detection of Ag^+ ions with a high sensitivity of 10 nM. MoS_2 sheets functionalized at their edges with thionin has also been shown to have stable electrochemical response to the presence of DNA with a linear decrease in electrochemical change occurring with increasing DNA concentration from 0.09 ng mL^{-1} to 1.9 ng mL^{-1} even in the presence of a relatively high concentration of protein [24]. Negatively charged polyxanthurenic acid functionalized MoS_2 sheets has also been shown by Yang et al. to experience a stronger adsorption of positively charged guanine and adenine, resulting in a highly electroactive platform for detection of guanine and adenine [29].

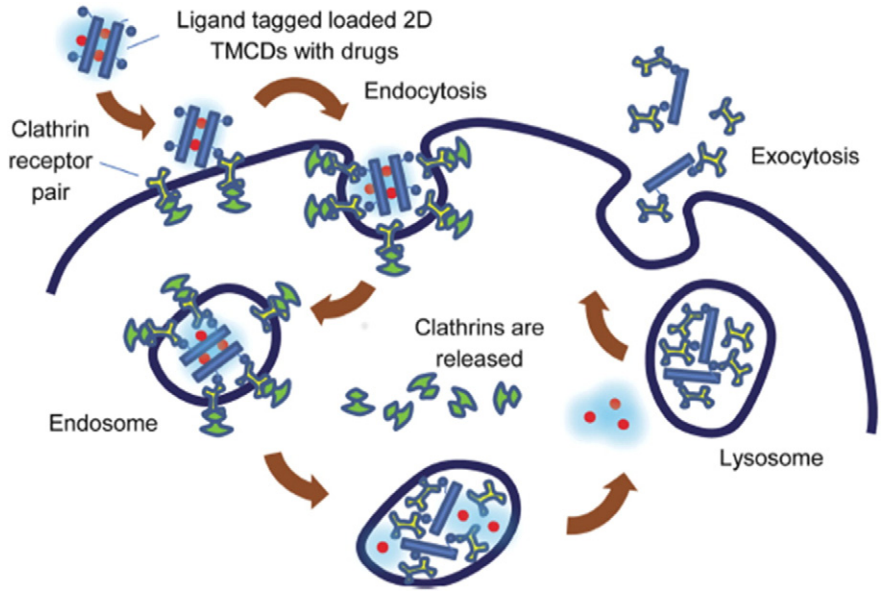

Fig. 4. Schematic illustration of drug delivery concept, where layered 2D TMDCs are loaded with drugs and conjugated with a ligand allowing cellular uptake. The ligand on the 2D TMDC anchors to the receptor-clathrin pair facilitating clathrin mediated endocytosis. The loaded 2D TMDC enters the cell within a vesicle. In the later stages of transport the drug is released either from the surface or from within the layers. In the final step, ideally the emptied 2D TMDCs are externalised via extocytosis (under environmental changes such as pH lowering). Reproduced with permission from Ref. [10]. Copyright 2015, WILEY-VCH Verlag GmbH & Co. KGaA, Weinheim.

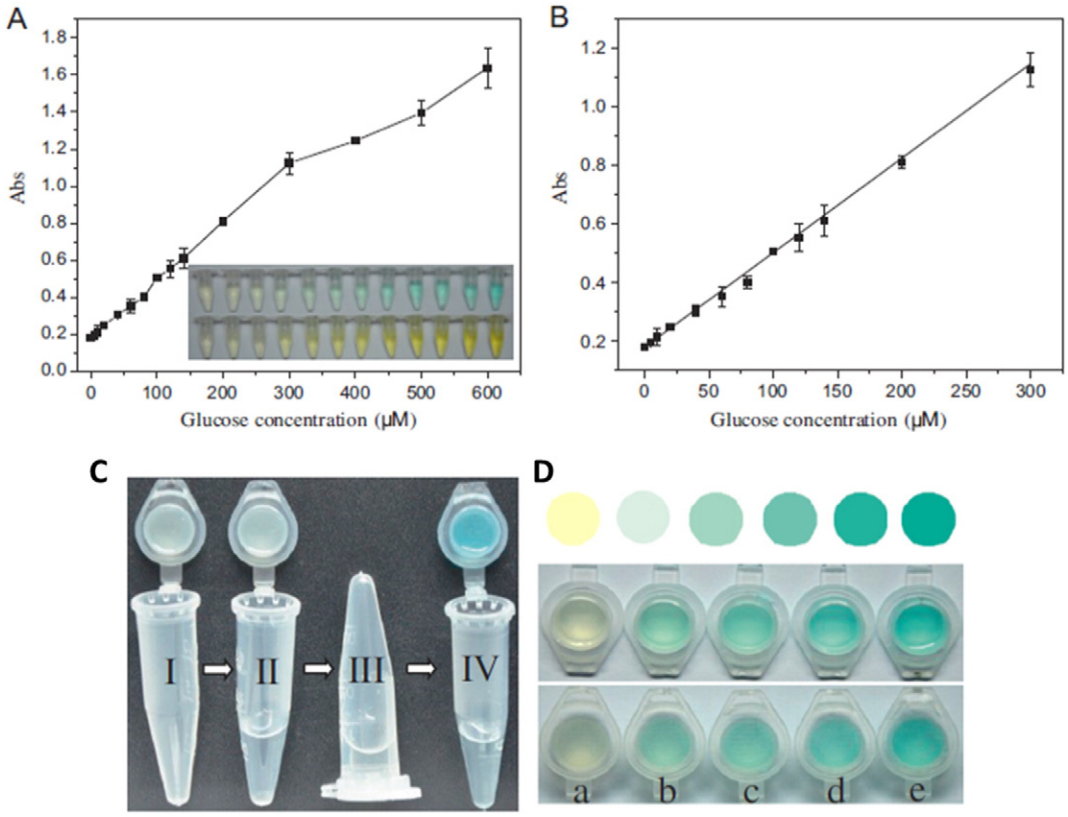

Fig. 5. A) A dose-response curve for glucose detection using WS_2 nanosheets as peroxidase mimics and B) the linear calibration plot for glucose. The error bars represent the standard deviation of three measurements. Inset of A) is a corresponding photo of the colored products without (top) and with (down) the addition of 50 mL 20% (V/V) sulfuric acid for different concentrations of glucose (μM) (from left to right: 0, 10, 20, 40, 60, 80, 100, 120, 140, 160, 200, 300). C) Procedure for the detection of glucose in serum samples. (I) Opening the snap cap of test kit (pale yellow color in the hydrogel), (II) adding diluted serum sample solution to the test kit, (III) closing the snap cap and turning upside down the test kit before incubation at 40 °C for 60 min, (IV) turning upside down the test kit again and opening the snap cap (blue color in the hydrogel). D) (top) Standard colorimetric cards for serum glucose (mM) (from left to right: 0, 4, 6, 8, 10, 12) and (bottom) photos of the hydrogel with different concentrations of serum glucose when opening the snap cap of the test kit (middle) and closing the snap cap of the test kit. The concentration of glucose (mM) in serum samples: (a) blank, (b) 5.31, (c) 6.98, (d) 8.49, (e) 11.88. Reproduced with permission from Ref. [28]. Copyright 2014, Elsevier V.B.

Lin et al. demonstrates in Fig. 5 that organic molecules such as 3,3′,5,5′-tetramethylbenzidine (TMB) can be used as visualizing reagents in conjunction with WS_2 nanosheets to allow visual detection of blood glucose [28]. This occurs due to the catalytic oxidation of TMB in the presence of H_2O_2 that results in a color reaction. Thus, in using a mixture of TMB, WS_2 nanosheets and glucose oxidase which produces H_2O_2 on reaction with glucose, a concentration dependent visual detection of blood glucose is made possible. A gradual change in color is observed as the glucose concentration is increased. Biomarkers based on the intrinsic photoluminescence of TMDCs can also be used for cell labeling. However, this is only possible after functionalization of molecules to imbue the TMDCs nanosheets with functional groups that allow dissolution in water and subsequent cellular uptake. Such modification was carried out by Anbazhagan et al., where thioglycolic acid was used as a stabilizer for MoS_2 nanosheets in water and the photoluminescence of the MoS_2 sheets were used to optically label human HeLa cancer cells without causing any cell necrosis [23].

Label free biosensors can be fashioned from functionalized TMDCs when used as field effect transistors. Detection of biological species occurs when they are bonded with the gate dielectric or conducting channel, the TMDCs, and a resultant modulation in conductance of the transistors is experienced [25–27]. To this end, Sarkar et al. has demonstrated indirect functionalization of MoS_2 through the attachment of biotin, a receptor molecule, onto the HfO_2 dielectric which is located above the MoS_2 layer [25]. Depending on whether the pH is greater or smaller than the isoelectric value at which the target molecule, streptavidin, is neutral, the current flowing through the MoS_2 at the same gate voltage applied decreases or increases accordingly. This occurs due to the additional gating effect exerted by the electrostatic interactions taking place when the biotin and streptavidin binds together. The biosensor is molecule specific as well because of the use of receptors which respond only to specific target molecules. Similar concept has also been reported by Lee et al. but with the receptor-target pair being anti-prostate specific antigen antibody and prostate specific antigen respectively with the MoS_2 layer being functionalized instead, allowing a detectable concentration of 1 pg/mL that is lower than the clinical cut off level of 4 ng mL^{-1} [26].

4.3. DNA-based functionalization

DNA is ubiquitous in almost every living organism and its detection and study is important in the biomedical field. Hence, it is desirable to develop cost-effective, selective and sensitive platforms for detection of DNA sequences with direct quantitative diagnostics. TMDC, being a relatively large surface area planar platform onto which ssDNA can be easily self-assembled on, has been recently applied in numerous DNA based probes. The large surface allows accommodation of a high density of sensing molecules to enable short assay duration as well as increase sensitivity. Self-assembly and interaction between the TMDC and the DNA biomolecules occurs through van der Waals forces between the nucleobases of the DNA and the basal surface of TMDCs [11,55]. The basic principle is the reduced interaction between ssDNA and the TMDC onto which it is assembled on after hybridization with a separate target complementary DNA strand [51–53]. Such a lifting of interaction can also occur for protein-based probes when protein/peptide complexes are formed [46,47]. The variation in interaction strengths between the ssDNA, target biochemical and the TMDC provides the mechanism around which the functionalization architecture for DNA based probe is designed.

A particular property of TMDC is its strong fluorescent (FL) quenching effect due to photo-induced electron transfer from the excited fluorescent agent to the TMDC before re-radiation can occur. This characteristic has been exploited recently by Zhu et al. (Fig. 6) through the fabrication of a homogenous assay format for DNA based on monolayer MoS_2 functionalized with dye-labeled DNA for the detection of a segment of *Homo sapiens* tumor suppressor gene p53 [53]. In their work, fluorescent dye-labeled (fluorescein) ssDNA (P1) of the exon segments for p53 is adsorbed onto the surface of MoS_2 nanosheets produced by liquid exfoliation. Due to the interaction between the ssDNA and MoS_2, fluorescence from the dye is quenched. When the complementary target DNA (T1) of the adsorbed ssDNA on MoS_2 is present, hybridization occurs between two of them, forming double stranded DNA and quenching of the fluorescence is reduced. Such a reduction is manifested in the increase in FL intensity after introduction of the target complementary DNA and this intensity forms the basis of a quantitative measure for the target DNA. This phenomenon occurs due to the decrease in interaction between the newly formed double-stranded DNA and the MoS_2 after hybridization has taken place. During hybridization, the nucleobases which were initially in contact with the MoS_2 surface is now nested between the densely negatively charged helical phosphate back bones, resulting in the lifting of the dye-labeled probe away from the MoS_2 surface and hence recovering its fluorescence. The detection limit of such a sensor is up to 500 pM with a detection timeframe of a few minutes, showing promise as a 2D-material based diagnostic tool.

Based on similar principles, a microfluidic system based approach is also demonstrated [52], having a smaller size and volume requirement, thus enhancing its efficiency. In this system, probe ssDNA, target DNA and MoS_2 nanosheets are made to flow through a zigzag micro channel and akin to previous reports, the extent of fluorescence retained provides quantitative analysis of the target DNA concentration. In this work, through application of microfluidic channels, attomolar levels of sensitivity are attained. Other fluorescence quenching based 2D TMDCs DNA sensors such as WS_2 [46,47,49], TiS_2 [51] and TaS_2 [51] nanosheets have also been developed.

The mechanism behind the quantitative sensing of a single sequence of DNA can also be extended to multiplex detection platforms by having different ssDNA probes present on the same TMDC surface. This has been shown by Zhang et al. where a single TMDC layer is functionalized with two separate fluorescent-labeled ssDNA probes that hybridize specifically to their respective target DNA sequences, namely the H1N1 subtype gene and H5N1 gene [51]. Due to the fluorescent labels having emissions of different wavelengths and the probes only hybridizing with their complementary target, selective detection of the target DNA is made possible, exhibiting the ability for multiplex DNA detection.

Other than complementary DNA, ssDNA functionalization can also be used to detect microRNAs. Recent studies by Xi et al. have shown that fluorescence from the dye labeled ssDNA probes functionalized on WS_2 nanosheets can be recovered in the presence of the corresponding miRNA of the DNA probe and the sensitivity can be enhanced in the presence of a DNA/RNA heteroduplex specific nuclease (DSN) [49]. The DSN serves to cleave the duplex, releasing the target miRNA for further hybridization with other ssDNA probes which results in repeated chain cycles of cleavage, release and hybridization, amplifying the fluorescence signal. This occurs as the shorter oligonucleotide fragments which were cleaved from the dye-labeled ssDNA probes have reduced affinity to WS_2 and therefore reduced quenching of their fluorescent signal. Due to the presence of DSN which is highly specific to the RNA/DNA heteroduplex, miRNA/ssDNA probe duplexes with single base pair mismatch will not be cleaved and thus the presence of a single base pair mismatch can be detected through the continued quenching of the fluorescent signal. Non-fluorescence based detection of DNA hybridization through electrochemical activity of ssDNA functionalized MoS_2 was demonstrated by Loo et al. in which the electrochemical behavior of MoS_2 nanoflakes varies in depending on the presence of ssDNA, hybridized double-stranded DNA or mismatched DNA pairs [35].

Other than biomolecules, using similar fluorescence quenching mechanisms, DNA functionalized TMDCs can also be employed to detect inorganic substances. Silver ions which are toxic to the human body in large quantities can also be detected through such platforms as they

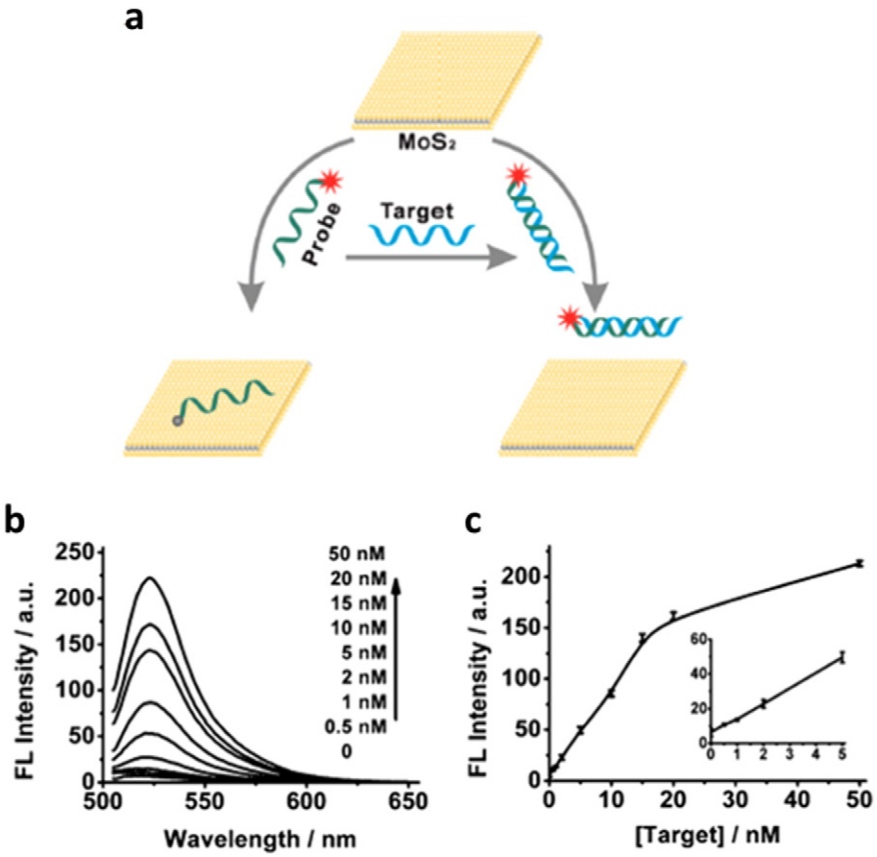

Fig. 6. a) Schematic illustration of the fluorimetric DNA sensing assay. b) Fluorescence spectra of P1 (15 nM) in the presence of different concentrations of T1 (0, 0.5, 1, 2, 5, 10, 15, 20, and 50 nM). (c) Calibration curve for DNA detection. Inset: amplification of the low concentration range of the calibration curve. Excitation and emission wavelengths are 494 and 520 nm, respectively. Reproduced with permission from Ref. [53]. Copyright 2013, American Chemical Society.

cause a self-folding of the fluorophore labeled ssDNA sequences that were adsorbed onto MoS_2, thereby weakening its affinity to the MoS_2 layer [30]. Likewise, a reverse approach for detection of toxic uranyl ions is also possible based on similar principles. Zhang et al. reports on fluorophore-labeled DNA enzymes which are weakly interacting with MoS_2 nanosheets being cleaved in the presence of uranyl ions, resulting in the release of the fluorophore fragments and subsequent fluorescence quenching [48]. Thus, through functionalization of TMDCs using biomolecules such as DNA and exploiting their variation in interaction, one is able to use these TMDC-based nanomaterials as a highly sensitive and rapid response diagnostic platform. Depending on the target to be detected, one can choose an appropriate probe to quantitatively detect both organic and inorganic chemicals.

4.4. 2D heterostructures

As mentioned in the previous section, MoS_2 decorated with DNA single strands which are labeled with fluorescent probes can be used in DNA diagnostics. Recent developments have allowed use of PL in TMDCs as the detection basis instead of depending on external fluorescent tagging of the probe. Such a device would entail the usage of 2D heterostructures formed by stacking individual 2D materials together. This is required to overcome the ultra-sensitivity of TMDCs to variations in the external environment such as extrinsic charge doping from chemical elements as it would make it difficult to determine small changes in an aqueous environment where varying amounts of oxygen and moisture is present. Such aqueous environment is commonly encountered as majority of the targets in biological systems require these media to survive. Therefore, through stacking of another inert 2D material such as graphene, high sensitivity of the TMDC to changes in target concentration can be maintained while ensuring that the integrity of the TMDC is intact over repeated usage.

Such a device is demonstrated recently by Loan et al. where a DNA hybridization based detector was constructed from a stacked MoS_2 graphene heterostructure (Fig. 7) [44]. In their work, graphene was stacked onto MoS_2 which was grown via CVD on sapphire. The graphene layer serves two functions, one being a protective layer to ensure that damage and the other for keeping perturbation to the MoS_2 from the external chemical environment limited while at the same time serving as a platform onto which the DNA probe can be immobilized and hosted. Due to partial electron charge transfer from the NH_2 group of the DNA bases to graphene, the probe DNAs are secured and even remained so after hybridization with their target complimentary DNA. Violent rinsing of the heterostructure based detector only removes the mismatched-DNAs while keeping the hybridized complimentary DNA pairs intact on the surface.

PL response intensity from the MoS_2 monolayer is then used as the basis for detection of target DNA and the results are shown in Fig. 7. An initial decoration of single stranded probe DNA does not cause significant change in the PL intensity. As the target DNA is hybridized with the probe strands, PL intensity increases with the target DNA concentration (Fig. 7a and c). Note that the sensitivity is able to reach attomolar levels of target DNA concentration. Furthermore, mismatched DNA pairs do not affect the PL intensity, as seen in Fig. 7b and 7d. The changes in PL are attributed to the increase in hole charge carrier doping in MoS_2 with an increased presence of negatively charged phosphate groups present in the target DNAs that still reside on the graphene surface after the mismatched pairs or strands are washed off.

Efforts have also been applied in functionalizing electrocatalytic TMDCs with other highly conductive 2D materials such as

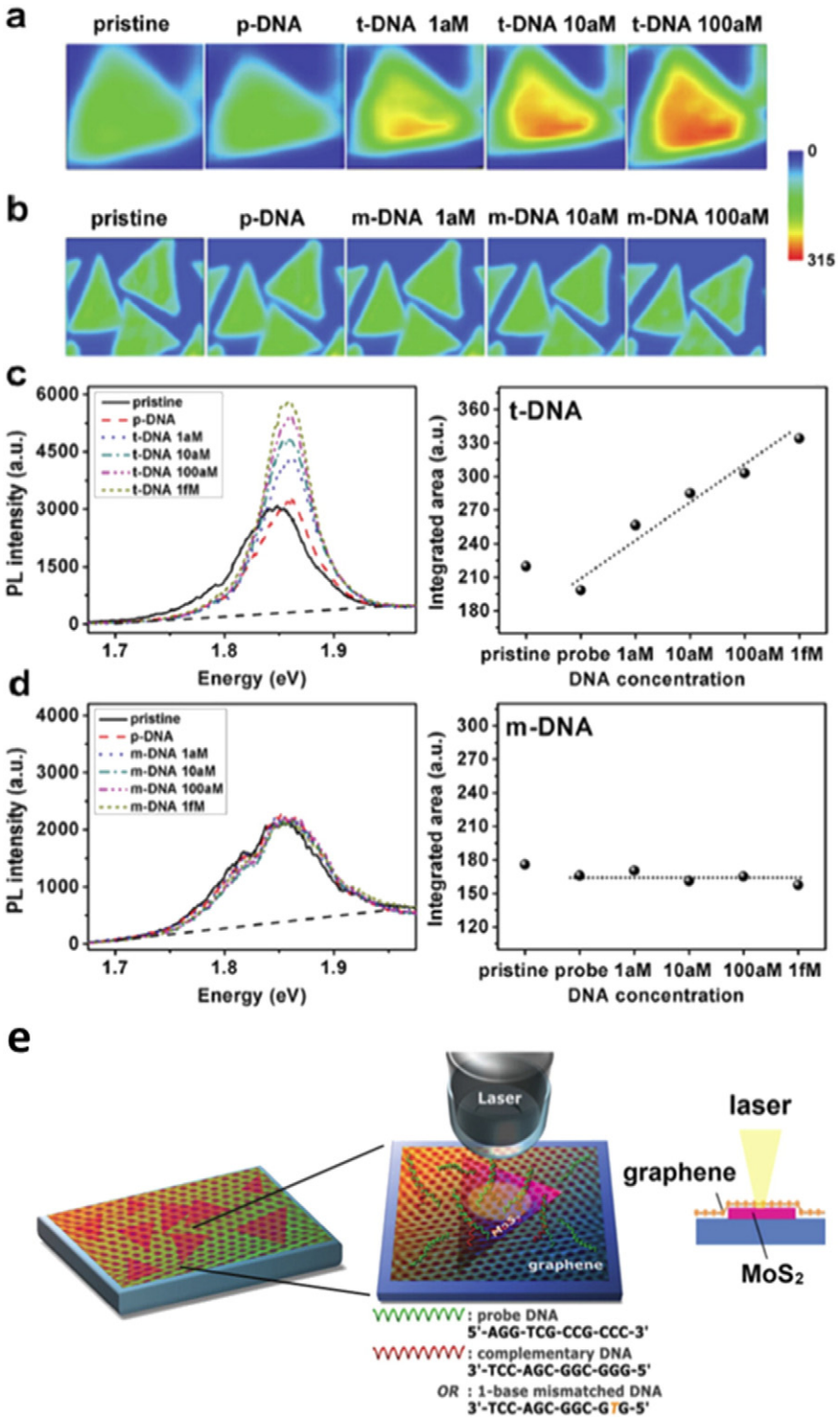

Fig. 7. PL peak area mappings of the graphene/MoS_2 heterostructure hybridized with a) the complementary target DNA and b) the mismatched DNA. The PL spectra and integrated PL peak area in the presence of c) target DNA (1, 10, 100, and 1000 aM) and d) mismatched DNA (1, 10, 100, and 1000 aM). e) Schematic of the DNA detection device. Reproduced with permission from Ref. [44]. Copyright 2014, WILEY-VCH Verlag GmbH & Co. KGaA, Weinheim.

graphene in order to enhance their effectiveness [37,38,42,45]. Heterostructure based nanocomposites such as MoS_2-graphene together with horseradish peroxidase can be used for electrochemical-based quantitative detection of hydrogen peroxide [45]. Other applications involve graphene-tungsten disulfide for detection of catechol, resorcinol and hydroquinone [37] as well as graphene-MoS_2 composites for acetaminophen sensing [38]. Such 2D material based heterostructures, though widely studied in the physical sciences, has also now been recently applied in biomedical applications. With proper selection from a diverse library of these 2D materials [64], such heterostructures could be extended into other areas that require highly sensitive detection such as proteins, metal-ion contamination in water or even monitoring of intra/extra-cellular activities. Furthermore, their planar nature ensures maximal interaction between dissimilar layers of 2D materials and allows for easy formation of heterostructures.

4.5. Metallic nanoparticles

Due to the presence of a large number of exposed catalytic edges in TMDC nanosheets which serve as catalytic sites for chemical reactions, they are commonly applied as electrochemical based biosensors [65]. One aspect of their attractiveness in using TMDCs is the distinctive cyclic voltammetric peaks that are observed during electrochemical reactions. To increase their sensitivity and efficacy in these electrochemical reactions, metallic nanoparticles are often added to serve as additional catalytic sites or create defects in the TMDC layer to increase the number of electroactive sites on the TMDC surface. In addition, they can serve as anchors on the TMDC surface to incorporate other functional materials. TMDC nanosheets can also form well-stabilized hierarchical composites easily with metal nanoparticles [36,66,67]. These metallic nanoparticles are generally introduced through an initial mixture of the respective chemical compounds such as $HAuCl_4$ [43] or copper chloride [40] with the TMDC in solution followed by chemical reduction of these compounds to form metallic nanoparticle-TMDC composites.

Recently, hemoglobin was immobilized on a gold-nanoparticle decorated MoS_2 nanosheet to serve as a hydrogen peroxide and nitric oxide sensor through the electrocatalytic reduction of the target chemicals (Fig. 8) [43]. The Au nanoparticles provide sites for immobilization of hemoglobin while simultaneously aiding electron transfer between the electrode and the electroactive center of the hemoglobin. During reduction of the target chemicals (H_2O_2 or NO), distinct redox peaks are characteristic to either chemicals are observed (Fig. 8), indicating that the hemoglobin retains its bioactivity even after immobilization on the Au—MoS_2 composite platform. Detection limits of 4 μM and 5 μM for H_2O_2 and NO are obtained respectively with linear increase (decrease) in reduction (oxidation) peaks with increasing amounts of these chemicals.

Au nanoparticle functionalized polymer/graphene-MoS_2 composite has also been reported for detection of eugenol, a compound used as flavoring agents or in fragrances but has adverse health effects beyond a 2.5 mg/kg intake [42]. Dopamine analysis was also carried out by a different group using Au nanoparticle decorated polyaniline-MoS_2 composites [41]. Other metallic elements include Cu nanoparticles functionalized MoS_2 nanosheets used for glucose detection [40] in which the presence of these nanoparticles generates an observable current response due to the oxidation of glucose as well as selectivity over other chemicals such as ascorbic acid, uric acid and dopamine. Similarly, Ni nanoparticles [31] can also form hybrids with MoS_2 for glucose detection with an even higher sensitivity of 1824 μA mM^{-1} compared to Cu (1055 μA mM^{-1}). Likewise, electrocatalytic oxidation of tryptophan was demonstrated using silver nanoparticle functionalized chitosan-MoS_2 composite [39]. TMDCs can also be functionalized with metallic nanoparticles which serve as anchors for addition of other materials for non-electrochemical purposes. This was demonstrated by Liu et al. where *meso*-2,3-dimercaptosuccinic acid (DMSA)-modified iron oxide nanoparticles are first self-assembled on MoS_2 nanosheets through bond formation of the sulfur present on the acid at the sulfur-vacancy defect sites present on the MoS_2 surface [15]. Subsequently, these nanoparticles were further functionalized by amino terminated PEG while the MoS_2 surface is modified by lipoic acid terminated PEG, ensuring high stability in the presence of glutathione, a thiol-containing molecule commonly found in physiological environments. The resultant nanocomposites were further labeled with 64Cu isotopes, allowing multi-modal imaging capabilities in a single system through strong paramagnetism of iron oxide nanoparticles for magnetic resonance imaging, strong NIR absorbance of MoS_2 for photoacoustic tomography and 64Cu based positron emission tomography. Furthermore, the strong NIR absorbance of MoS_2 enables photothermal therapy on the targeted tissue. Thus through appropriate functionalization of particular metallic nanoparticles, one can enhance catalytic behavior of TMDC nanosheets to allow better monitoring of electrochemical reactions for biosensing or serve as anchors for further accommodation of materials to allow multi-functional capabilities.

4.6. Nanopores

In the past, single nucleotide identification [68,69] and DNA sequencing [70] have been carried out using biological based nanopores such as proteins or lipid membranes. In these systems, nucleotide detection and sequencing is done by monitoring the ionic current variation through the nanopore as an electric field drives DNA translocation through it. A drawback of using such biological pores is their structural fragility as well as additional biochemical that are required to modify them. Furthermore, the thicknesses of these nanopores are generally in the order of 10–20 nm, limiting the spatial resolution to 30–60 nucleotide units at a time [71]. Thus, through use of 2D-TMDCs which can be as thin as 0.7 nm, one could potentially reduce the SNR of the ionic current. An additional advantage in using TMDC based nanopore is the additional channel of detection through the monitoring of electronic

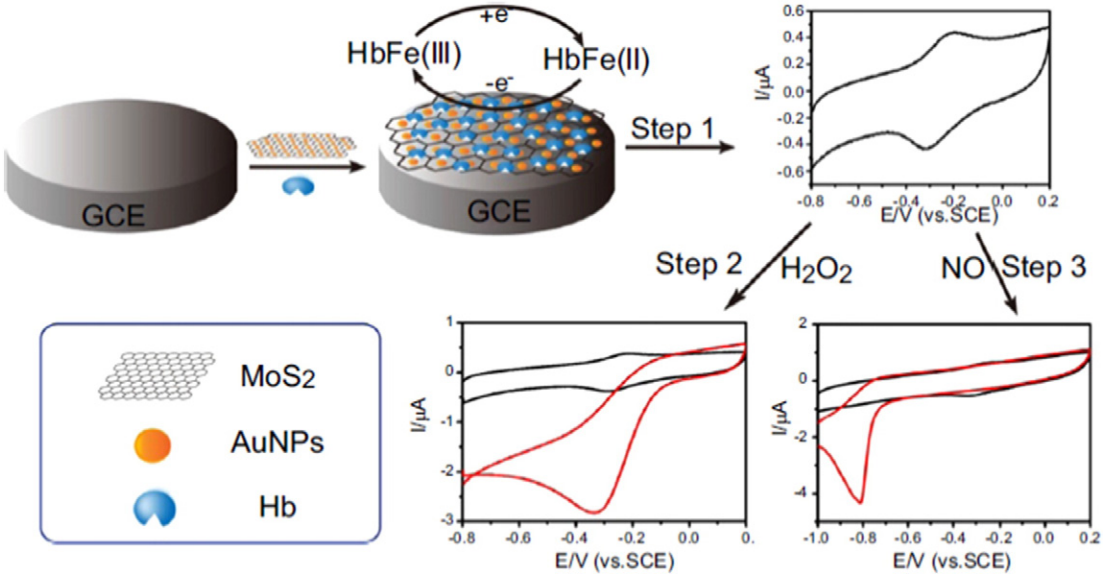

Fig. 8. Schematic diagram of Hb–Au nanoparticles on MoS_2/Glassy Carbon Electrode (GCE) fabrication process. (Step 1) Direct electrochemistry of Hb at Au nanoparticles on MoS_2 nanocomposite film modified electrode. (Step 2) and (Step 3) Hb–Au nanoparticles on MoS_2/GCE electrocatalytic reduction toward H_2O_2 and NO, respectively. Reproduced with permission from Ref. [43]. Copyright 2015, IOP Publishing Ltd.

current passing along the TMDC layer itself during DNA translocation. In light of this, MoS_2 monolayer has been decorated with nanopores for nucleotide detection and their viability have been theoretically and experimentally proven recently [32–34].

Recently, Feng et al. has demonstrated single-nucleotide identification using nanopores created in MoS_2 monolayer through the use of a viscosity gradient in the ionic liquid which allows regulation of the translocation speed [32]. A SNR of up to 16 was also achieved in such nanostructures with pores as small as 2 nm. The nanopores were fabricated by irradiation of the target location using transmission electron microscope and these pores require no additional functionalization for detection of DNA translocation. Unlike nanopores in other 2D materials such as graphene where clogging can occur on pristine graphene surfaces [72], the interaction and sticking of the DNA to the pores is reduced by the presence of the Mo-rich region around the drilled pore.

The device schematic and TEM of the nanopore used are shown in Fig. 9a and b [32]. As solid state nanopores instead of biological ones are used, the size of the nanopore can be easily adjusted as it is created using an external irradiation. Fig. 9c and d describes the variation in ionic current through the nanopore for different homopolymers made up of a chain of identical nucleotides as well as single nucleotides respectively. The current drop that occurs as each chain passes through the pore is unique to the particular constituent nucleotide (Fig. 9c), indicating specificity in nucleotide detection while to a certain extent (Fig. 9d), single nucleotide detection is exhibited. Hence, in contrast to the previous sections where different functional materials are added to TMDCS, one can also destructively functionalize TMDC by creating nanopores in them and exploit the unique 2D nature of TMDCs for highly sensitive DNA sequencing.

5. Conclusion and outlook

In our discussion, we have shown that through appropriate functionalization, TMDCs can be tailored to serve a wide range of biomedical applications. The different chemical species that are compatible with TMDCs vary from large molecules such as polymers to smaller organic molecules and even to biomolecules like DNA or metallic nanoparticles. Due to their unique physicochemical properties, functionalized TMDCs have demonstrated to be effective drug delivery carriers, therapeutic agents, diagnostic platforms as well as biosensing. However, certain key obstacles are still present in the proliferation of their application in biological systems. Firstly, consistency in the synthesis of these materials has not been completely achieved yet. There is currently no standard synthesis technique that can produce functionalized TMDCs with well controlled dispersity, material thickness and dimensions as well as uniformity in

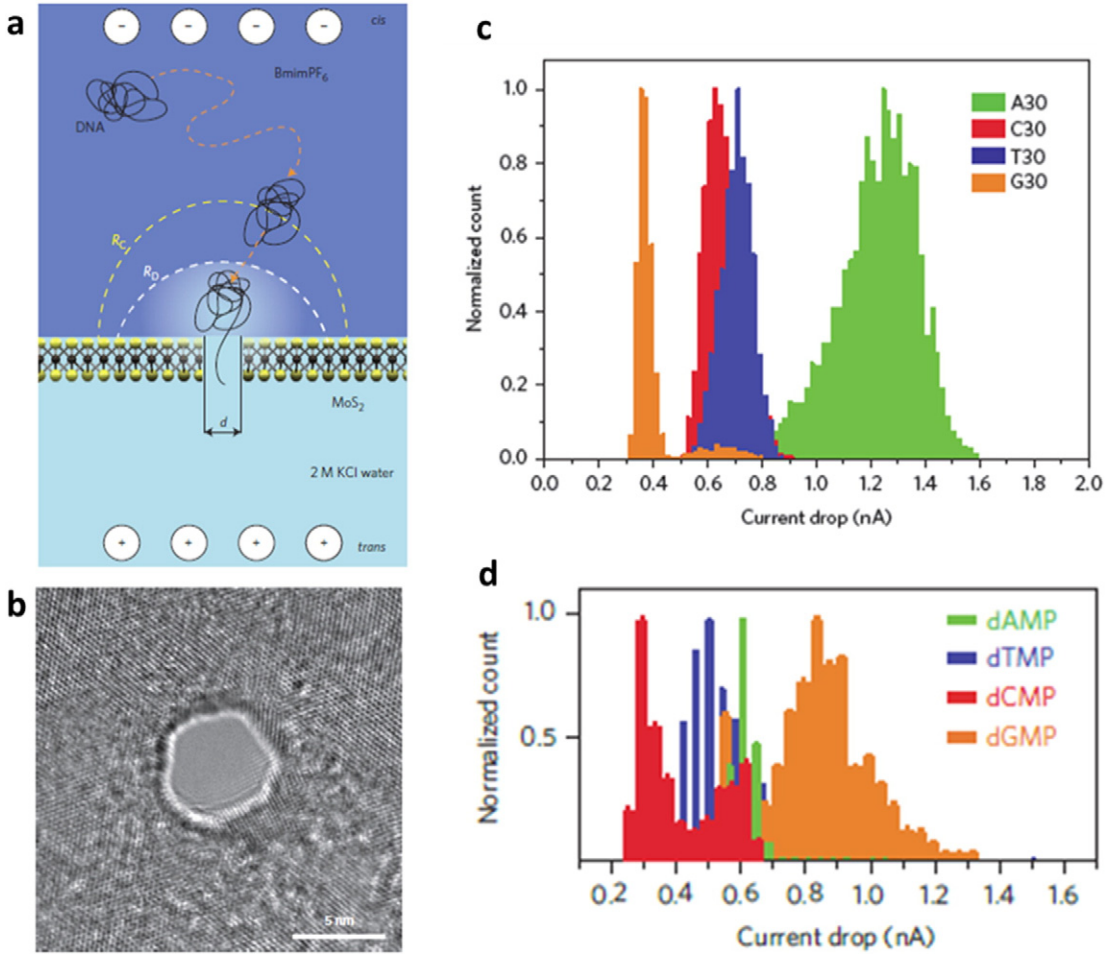

Fig. 9. a) The cis chamber contains RTILs ($BmimPF_6$) and the trans chamber contains 2 M aqueous KCl solution. The two chambers are separated by a monolayer MoS_2 membrane with a nanopore. The schematic also shows the dynamics of DNA translocation through a nanopore. Away from the pore, DNA motion is purely diffusive due to the negligible electric field, but once within the area of the capture radius R_c, DNA will be accelerated toward the pore by a force due to electrophoretic and electroosmotic effects. Part of the DNA will undergo conformational change and one end will dive into the pore. The non-translocated part of the DNA polymer–monomers will keep the coil conformation and experience a strong Stokes dragging force from the ionic liquids. Consequently, DNA translocation through the pore can be significantly slowed. b) Bright-field transmission electron microscope (TEM) image of a 5 nm solid-state pore fabricated in a monolayer MoS_2 membrane suspended over a 200 × 200 nm^2 etched area formed in the center of a 20 μm low-stress SiNx membrane with a thickness of 20 nm. c) Normalized histogram of current drops for each DNA homopolymer. Mean values: poly A30, 1.25 ± 0.12 nA; poly C30, 0.64 ± 0.07 nA; poly T30, 0.71 ± 0.06 nA; poly G30, 0.36 ± 0.03 nA. d) Normalized histogram of current drops for dAMP, dTMP, dCMP and dGMP. Reproduced with permission from Ref. [32]. Copyright 2015, Macmillan Publishers Ltd.

functionalization across the material surface. Current methods for large scale synthesis of TMDC nanosheets involve exfoliation from their bulk crystals, resulting in a wide distribution in size and thicknesses while bottom-up synthesis which can produce well controlled thicknesses of TMDC face difficulty in converting to well-functionalized nanosheets.

Furthermore, though cytotoxicity of TMDCs in biological systems is shown to be relatively low, the mechanisms taking place before and after its cellular uptake or use as therapeutic agent have not been completely understood yet, especially its bio-distribution, degradation in the body and its subsequent excretion. Toxicity to non-targeted areas of the biological system has also not been rigorously studied yet and will be essential before any clinical trials can take place. 2D materials other than TMDCs such as BN and graphene can also be functionalized for use in biological systems and may prove useful when employed in tandem with TMDCs. Currently functionalization of TMDCs for biomedical applications is still in its nascent stages but has shown much potential as a new nanomaterial for synergistic therapy, multi-modal imaging, highly sensitive biosensing and externally controlled in vivo drug release agent which is difficult to be replicated by current biodegradable materials like liposomes, nanocrystals, micelles and hydrogels [73–82]. Hence, there exists both great promise as well as additional work to be carried out on the functionalization of TMDCs to make it a truly viable nanomaterial for biomedical applications.

Acknowledgement

The authors gratefully acknowledge financial support from the Institute of Materials Research and Engineering (IMRE) (Ubiquitous Electronics: The Case For Semiconductor 2D Materials, Large Area Growth of Atomically Thin 2D Semiconductors (CVD/PVD), No.: 1527000012) under the Agency for Science, Technology, and Research (A*STAR).

References

[1] K.S. Novoselov, A.K. Geim, S. Morozov, D. Jiang, Y. Zhang, S. Dubonos, I. Grigorieva, A. Firsov, Science 306 (2004) 666–669.
[2] S.L. Wong, H. Huang, Y. Wang, L. Cao, D. Qi, I. Santoso, W. Chen, A.T.S. Wee, ACS Nano 5 (2011) 7662–7668.
[3] H. Huang, D. Wei, J. Sun, S.L. Wong, Y.P. Feng, A.C. Neto, A.T.S. Wee, Sci. Rep. 2 (2012).
[4] H. Huang, S.L. Wong, C.-C. Tin, Z.Q. Luo, Z.X. Shen, W. Chen, A.T.S. Wee, J. Appl. Phys. 110 (2011) 014308.
[5] S.L. Wong, H. Huang, W. Chen, A.T. Wee, MRS Bull. 37 (2012) 1195–1202.
[6] S.L. Wong, K.H. Khoo, S.Y. Quek, A.T.S. Wee, J. Phys. Chem. C (2015).
[7] D. Jariwala, V.K. Sangwan, L.J. Lauhon, T.J. Marks, M.C. Hersam, ACS Nano 8 (2014) 1102–1120.
[8] Q.H. Wang, K. Kalantar-Zadeh, A. Kis, J.N. Coleman, M.S. Strano, Nat. Nanotechnol. 7 (2012) 699–712.
[9] K. Kalantar-Zadeh, J.Z. Ou, ACS Sens. (2015).
[10] K. Kalantar-Zadeh, J.Z. Ou, T. Daeneke, M.S. Strano, M. Pumera, S.L. Gras, Adv. Funct. Mater. 25 (2015) 5086–5099.
[11] Y. Chen, C. Tan, H. Zhang, L. Wang, Chem. Soc. Rev. 44 (2015) 2681–2701.
[12] G. Yang, C. Zhu, D. Du, J. Zhu, Y. Lin, Nanoscale 7 (2015) 14217–14231.
[13] B. Radisavljevic, A. Radenovic, J. Brivio, V. Giacometti, A. Kis, Nat. Nanotechnol. 6 (2011) 147–150.
[14] M. Chhowalla, H.S. Shin, G. Eda, L.-J. Li, K.P. Loh, H. Zhang, Nat. Chem. 5 (2013) 263–275.
[15] T. Liu, S. Shi, C. Liang, S. Shen, L. Cheng, C. Wang, X. Song, S. Goel, T.E. Barnhart, W. Cai, ACS Nano 9 (2015) 950–960.
[16] L. Cheng, J. Liu, X. Gu, H. Gong, X. Shi, T. Liu, C. Wang, X. Wang, G. Liu, H. Xing, Adv. Mater. 26 (2014) 1886–1893.
[17] S. Wang, Y. Chen, X. Li, W. Gao, L. Zhang, J. Liu, Y. Zheng, H. Chen, J. Shi, Adv. Mater. 27 (2015) 7117–7122.
[18] W. Yin, L. Yan, J. Yu, G. Tian, L. Zhou, X. Zheng, X. Zhang, Y. Yong, J. Li, Z. Gu, ACS Nano 8 (2014) 6922–6933.
[19] T. Liu, C. Wang, X. Gu, H. Gong, L. Cheng, X. Shi, L. Feng, B. Sun, Z. Liu, Adv. Mater. 26 (2014) 3433–3440.
[20] Y. Yong, L. Zhou, Z. Gu, L. Yan, G. Tian, X. Zheng, X. Liu, X. Zhang, J. Shi, W. Cong, Nanoscale 6 (2014) 10394–10403.
[21] X. Qian, S. Shen, T. Liu, L. Cheng, Z. Liu, Nanoscale 7 (2015) 6380–6387.
[22] N. Wang, F. Wei, Y. Qi, H. Li, X. Lu, G. Zhao, Q. Xu, ACS Appl. Mater. Interfaces 6 (2014) 19888–19894.
[23] R. Anbazhagan, H.-J. Wang, H.-C. Tsai, R.-J. Jeng, RSC Adv. 4 (2014) 42936–42941.
[24] T. Wang, R. Zhu, J. Zhuo, Z. Zhu, Y. Shao, M. Li, Anal. Chem. 86 (2014) 12064–12069.
[25] D. Sarkar, W. Liu, X. Xie, A.C. Anselmo, S. Mitragotri, K. Banerjee, ACS Nano 8 (2014) 3992–4003.
[26] J. Lee, P. Dak, Y. Lee, H. Park, W. Choi, M.A. Alam, S. Kim, Sci. Rep. 4 (2014).
[27] L. Wang, Y. Wang, J.I. Wong, T. Palacios, J. Kong, H.Y. Yang, Small 10 (2014) 1101–1105.
[28] T. Lin, L. Zhong, Z. Song, L. Guo, H. Wu, Q. Guo, Y. Chen, F. Fu, G. Chen, Biosens. Bioelectron. 62 (2014) 302–307.
[29] X. Luo, K. Jiao, J. Mater. Chem. B (2015).
[30] Y. Yang, T. Liu, L. Cheng, G. Song, Z. Liu, M. Chen, ACS Appl. Mater. Interfaces 7 (2015) 7526–7533.
[31] J. Huang, Y. He, J. Jin, Y. Li, Z. Dong, R. Li, Electrochim. Acta 136 (2014) 41–46.
[32] J. Feng, K. Liu, R.D. Bulushev, S. Khlybov, D. Dumcenco, A. Kis, A. Radenovic, Nat. Nanotechnol. 10 (2015) 1070–1076.
[33] A.B. Farimani, K. Min, N.R. Aluru, ACS Nano 8 (2014) 7914–7922.
[34] K. Liu, J. Feng, A. Kis, A. Radenovic, ACS Nano 8 (2014) 2504–2511.
[35] A.H. Loo, A. Bonanni, A. Ambrosi, M. Pumera, Nanoscale 6 (2014) 11971–11975.
[36] M. Pumera, A.H. Loo, TrAC Trends Anal. Chem. 61 (2014) 49–53.
[37] K.-J. Huang, L. Wang, Y.-J. Liu, T. Gan, Y.-M. Liu, L.-L. Wang, Y. Fan, Electrochim. Acta 107 (2013) 379–387.
[38] K.-J. Huang, L. Wang, J. Li, Y.-M. Liu, Sensors Actuators B Chem. 178 (2013) 671–677.
[39] X. Xia, Z. Zheng, Y. Zhang, X. Zhao, C. Wang, Sensors Actuators B Chem. 192 (2014) 42–50.
[40] J. Huang, Z. Dong, Y. Li, J. Li, W. Tang, H. Yang, J. Wang, Y. Bao, J. Jin, R. Li, Mater. Res. Bull. 48 (2013) 4544–4547.
[41] K.-J. Huang, J.-Z. Zhang, Y.-J. Liu, L.-L. Wang, Sensors Actuators B Chem. 194 (2014) 303–310.
[42] Q. Feng, K. Duan, X. Ye, D. Lu, Y. Du, C. Wang, Sensors Actuators B Chem. 192 (2014) 1–8.
[43] J. Chao, M. Zou, C. Zhang, H. Sun, D. Pan, H. Pei, S. Su, L. Yuwen, C. Fan, L. Wang, Nanotechnology 26 (2015) 274005.
[44] P.T.K. Loan, W. Zhang, C.T. Lin, K.H. Wei, L.J. Li, C.H. Chen, Adv. Mater. 26 (2014) 4838–4844.
[45] H. Song, Y. Ni, S. Kokot, Biosens. Bioelectron. 56 (2014) 137–143.
[46] S. Wang, Y. Zhang, Y. Ning, G.-J. Zhang, Analyst 140 (2015) 434–439.
[47] Y. Yuan, R. Li, Z. Liu, Anal. Chem. 86 (2014) 3610–3615.
[48] H. Zhang, Y. Ruan, L. Lin, M. Lin, X. Zeng, Z. Xi, F. Fu, Spectrochim. Acta A Mol. Biomol. Spectrosc. 146 (2015) 1–6.
[49] Q. Xi, D.-M. Zhou, Y.-Y. Kan, J. Ge, Z.-K. Wu, R.-Q. Yu, J.-H. Jiang, Anal. Chem. 86 (2014) 1361–1365.
[50] C. Tan, P. Yu, Y. Hu, J. Chen, Y. Huang, Y. Cai, Z. Luo, B. Li, Q. Lu, L. Wang, J. Am. Chem. Soc. 137 (2015) 10430–10436.
[51] Y. Zhang, B. Zheng, C. Zhu, X. Zhang, C. Tan, H. Li, B. Chen, J. Yang, J. Chen, Y. Huang, Adv. Mater. 27 (2015) 935–939.
[52] H. Yinxi, S. Yumeng, H. Ying Yang, A. Ye, Nanoscale 7 (2015) 2245–2249.
[53] C. Zhu, Z. Zeng, H. Li, F. Li, C. Fan, H. Zhang, J. Am. Chem. Soc. 135 (2013) 5998–6001.
[54] C. Tan, H. Zhang, Chem. Soc. Rev. 44 (2015) 2713–2731.
[55] X.P. He, H. Tian, Small (2015).
[56] S.S. Chou, B. Kaehr, J. Kim, B.M. Foley, M. De, P.E. Hopkins, J. Huang, C.J. Brinker, V.P. Dravid, Angew. Chem. 125 (2013) 4254–4258.
[57] X. Huang, Z. Zeng, H. Zhang, Chem. Soc. Rev. 42 (2013) 1934–1946.
[58] Q. Ji, Y. Zhang, Y. Zhang, Z. Liu, Chem. Soc. Rev. (2015).
[59] Y. Shi, H. Li, L.-J. Li, Chem. Soc. Rev. (2015).
[60] H. Liu, S. Wong, D. Chi, Chem. Vap. Depos. 21 (2015) 241–259.
[61] S.S. Chou, M. De, J. Kim, S. Byun, C. Dykstra, J. Yu, J. Huang, V.P. Dravid, J. Am. Chem. Soc. 135 (2013) 4584–4587.
[62] J.-S. Kim, H.-W. Yoo, H.O. Choi, H.-T. Jung, Nano Lett. 14 (2014) 5941–5947.
[63] B. Tian, C. Wang, S. Zhang, L. Feng, Z. Liu, ACS Nano 5 (2011) 7000–7009.
[64] A. Geim, I. Grigorieva, Nature 499 (2013) 419–425.
[65] S.M. Ahmed, H. Gerischer, Electrochim. Acta 24 (1979) 705–711.
[66] X. Huang, Z. Zeng, S. Bao, M. Wang, X. Qi, Z. Fan, H. Zhang, Nat. Commun. 4 (2013) 1444.
[67] L. Yuwen, F. Xu, B. Xue, Z. Luo, Q. Zhang, B. Bao, S. Su, L. Weng, W. Huang, L. Wang, Nanoscale 6 (2014) 5762–5769.
[68] Y. Astier, O. Braha, H. Bayley, J. Am. Chem. Soc. 128 (2006) 1705–1710.
[69] J. Clarke, H.-C. Wu, L. Jayasinghe, A. Patel, S. Reid, H. Bayley, Nat. Nanotechnol. 4 (2009) 265–270.
[70] A.H. Laszlo, I.M. Derrington, B.C. Ross, H. Brinkerhoff, A. Adey, I.C. Nova, J.M. Craig, K.W. Langford, J.M. Samson, R. Daza, Nat. Biotechnol. (2014).
[71] D. Branton, D.W. Deamer, A. Marziali, H. Bayley, S.A. Benner, T. Butler, M. Di Ventra, S. Garaj, A. Hibbs, X. Huang, Nat. Biotechnol. 26 (2008) 1146–1153.
[72] B.S. Husale, S. Sahoo, A. Radenovic, F. Traversi, P. Annibale, A. Kis, Langmuir 26 (2010) 18078–18082.
[73] Z. Li, D. Yuan, G. Jin, B.H. Tan, C. He, ACS Appl. Mater. Interfaces (2015), http://dx.doi.org/10.1021/acsami.1025b09822.
[74] Z. Li, H. Yin, Z. Zhang, K.L. Liu, J. Li, Biomacromolecules 13 (2012) 3162–3172.
[75] Z. Li, Z. Zhang, K.L. Liu, X. Ni, J. Li, Biomacromolecules 13 (2012) 3977–3989.
[76] X. Su, M.J. Tan, Z. Li, M. Wong, L. Rajamani, G. Lingam, X.J. Loh, Biomacromolecules 16 (2015) 3093–3102.
[77] Z. Li, X.J. Loh, Chem. Soc. Rev. 44 (2015) 2865–2879.
[78] Z. Li, J. Li, J. Phys. Chem. B 117 (2013) 14763–14774.
[79] Z. Li, D. Yuan, X. Fan, B.H. Tan, C. He, Langmuir 31 (2015) 2321–2333.
[80] Z. Li, B.H. Tan, Mater. Sci. Eng. C 45 (2014) 620–634.
[81] Z. Li, B.H. Tan, G. Jin, K. Li, C. He, Polym. Chem. 5 (2014) 6740–6753.
[82] Z. Li, L. Wu, in: W. Linping (Ed.), Polyhydroxyalkanoates (PHAs): Biosynthesis, Industrial Production and Applications in Medicine, Nova Science Publishers, USA 2014, pp. 181–217.